

Evaluating damage scale model of concrete materials using test data

Tesfaye A. Mohammed^a and Azadeh Parvin^{*}

Department of Civil Engineering, The University of Toledo, OH, USA

(Received November 23, 2012, Revised February 25, 2013, Accepted April 18, 2013)

Abstract. A reliable concrete constitutive material model is critical for an accurate numerical analysis simulation of reinforced concrete structures under extreme dynamic loadings including impact or blast. However, the formulation of concrete material model is challenging and entails numerous input parameters that must be obtained through experimentation. This paper presents a damage scale analytical model to characterize concrete material for its pre- and post-peak behavior. To formulate the damage scale model, statistical regression and finite element analysis models were developed leveraging twenty existing experimental data sets on concrete compressive strength. Subsequently, the proposed damage scale analytical model was implemented in the finite element analysis simulation of a reinforced concrete pier subjected to vehicle impact loading and the response were compared to available field test data to validate its accuracy. Field test and FEA results were in good agreement. The proposed analytical model was able to reliably predict the concrete behavior including its post-peak softening in the descending branch of the stress-strain curve. The proposed model also resulted in drastic reduction of number of input parameters required for LS-DYNA concrete material models.

Keywords: concrete material model; damage scale model; finite element analysis; LS-DYNA; reinforced concrete structure; bridge column; dynamic load; impact load; blast; vehicle impact

1. Introduction

In recent years, engineers' attention and concern have been drawn to safer design of structures under ballistic, blast, and impact loadings. Concrete is one of the widely used construction material in civil infrastructure. Nonlinear implicit and explicit finite element analysis (FEA) modeling offers a fast, reliable, and cost effective solution to investigate the behavior of reinforced concrete structures as opposed to time consuming and costly full-scale testing. However, in FEA modeling accurate material models are essential in capturing their true behavior under various loading conditions. For short duration and high impact load scenarios such as blast and vehicular impact, FEA modeling of reinforced concrete structures poses significant challenge and complexity and requires a dedicated explicit nonlinear FEA software program such as LS-DYNA.

Concrete material model characterization has been studied for quite some time (Buyukozturk and Shareef 1985, Han and Chen 1987, Hu and Schnobrich 1989, Malvar *et al.* 1997, Liu *et al.*

^{*}Corresponding author, Associate Professor, E-mail: aparvin@eng.utoledo.edu

^aPh.D. Student

2011), but due to its complex nonlinear behavior, a simple and yet accurate constitutive model has not been formulated. A few complex concrete material models with multiple input parameters have been widely used for explicit dynamic analysis of concrete structures using LS-DYNA and AUTODYN software programs subjected to severe shock and impact loading (Yonten *et al.* 2005, Tu and Lu 2009). The number of required input in these models ranges from 32 to 78 parameters.

When concrete is subjected to an increasing load situation, it undergoes various levels of damage, ranging from formation of cracks to ultimate failure. A damage function indicates the location of the current yield surface relative to limit surface and is a function of an effective plastic strain. Yonten *et al.* (2005) used a cylinder compressive strength test data and a vehicle road side barrier crash test data to evaluate various concrete material models labeled as MAT16, MAT25, MAT72 and MAT78 in LS-DYNA. The selected concrete cylinder test employed to assess the material models, was limited to high compressive strength concrete ($f'_c = 100 \text{ MPa}$) as opposed to normal strength concrete commonly used in buildings, bridges and road side barriers. Damage model parameters calculated for high-strength concrete were recalibrated by trial and error to obtain reasonable values for the case of normal-strength concrete. Their findings revealed that MAT16 exhibited superior performance as compared to other concrete material models, and concrete damage scale factor (η) and effective plastic strain (λ) input were essential variables controlling the concrete stress-strain softening response. They concluded that the stress-strain curve empirical data and damage scale model are critical in the material model which in turn influences the accuracy of the finite element analysis results.

Tu and Lu (2009) investigated concrete and concrete-like brittle material models in LS-DYNA and AUTODYN explicit nonlinear finite element analysis software programs. Material models MAT5, MAT17, MAT25, MAT72, MAT78, MAT96 in LS-DYNA, and JH, GR and RHT in AUTODYN were evaluated. The performance of these models was assessed by comparison of finite element analysis model and experimental results of a reinforced concrete slab subjected to blast loading. The authors concluded that the accuracy of the finite element results relied on the selection of material model as well as the input parameter values. They also emphasized that the damage scale factor (η) and effective plastic strain (λ) are crucial factors governing the general shape of the concrete stress-strain post peak softening behavior. It was concluded that the finite element analysis results of the slab under the blast loading showed unrealistic slow stress softening behavior when using RHT concrete material model with default parameter values. Their findings revealed that the selection of MAT72 in the simulation analysis provided a satisfactory and consistent response for the concrete material.

Mathematical formulation of this damage process is essential in order to capture the residual strength and serviceability of the damaged concrete. Thus, an accurate determination of concrete damage model plays a central role in nonlinear dynamic finite element analysis of concrete structures. Because the damage model is closely tied to the residual strength reserve of a member after it has undergone large inelastic load cycles (Chung *et al.* 1989).

Currently, for the existing concrete material models in LS-DYNA users can either adopt the default values included in the LS-DYNA material database, or input the damage model parameters manually. There are disadvantages associated with each method of inputting damage parameters; default values lead to inaccurate results, since they are not determined for all ranges of material properties. On the other hand, to manually input the damage model parameters is time consuming requiring a series of calculation to attain these parameters. As a brief description, in MAT_159_CSCM_CONCRETE formulation, damage accumulation is based upon two distinct formulations for brittle and ductile damage. Each of the brittle and ductile damage equations

requires two different input parameters that set the shape of the descending part of the constitutive model for the concrete behavior. MAT72REL3 requires a set of 13 input parameters to construct the damage function. These values are introduced as η_{01} to η_{13} as scale factors and λ_{01} to λ_{13} as damage function values. For MAT16 based on mode of response, either three constants must be defined to determine two yield surfaces and to account for damage in the material model or the damage function must be prescribed by a series of η and λ values (Livermore Software Technology Corporation 2012).

The present investigation proposes an analytical damage scale model to accurately characterize the concrete material post peak softening behavior. It also reduces total number of input parameters which users have to provide in MAT16, MAT84, MAT72rel3 and MAT159, the available concrete material options, in LS-DYNA explicit FEA program. Single-element FEA followed by statistical regression were developed using twenty experimental data sets reported in six previous studies (Rokugo and Koyanagi 1992, Jansen and Shah 1997, Ansari and Li 1998, Yi *et al.* 2003, Ren *et al.* 2008, Saatci and Vecchio 2009) on concrete compressive strength to formulate the concrete damage scale analytical model. Additionally, the accuracy of the proposed damage scale analytical model was validated through full-scale finite element model of a 13.4 m three-lane wide and 7.9 m high single hammerhead reinforced concrete bridge pier subjected to a truck impact load. The full-scale finite element model simulation results were compared to the field crash test data obtained from the collision of the truck with a rigid concrete barrier. Details of material models investigation using single-element FEA, proposed damage scale model, and full-scale bridge pier FEA model case study are presented in the following sections.

2. Material models investigation: calibration of single-element finite element analysis with experiments

In this section calibration of the single-element finite element analysis through existing concrete compressive test results reported in the literature is discussed. The FE models were calibrated for different concrete compressive strengths so that, the stress versus strain curves were in good agreement with those from experiments. The single-element analysis results were employed to obtain the damage scale model for each experiment.

Single element finite element model development eliminates complex structural effects such as closed or open crack mapping and mesh interlocking and assists to investigate the behavior of a material model that contains post peak softening region. A Solid164 element defined as a cube with side dimensions equal to 25.4 mm was used for the single element model. Zero displacement translational boundary condition was set for the bottom four nodes. A downward 1 mm displacement load was applied normal to the four nodes at the top face of the cube.

Twenty experimental data sets on concrete compressive strength specimens from six different studies were selected to calibrate the relationship between the concrete damage scale factor and the effective plastic strain of the single element model (Table 1). Default damage scale values suggested by the LS-DYNA software program were used as initial input and iteratively modified until the results of single element analysis and compressive strength experimental results agreed. In these experimental studies, concrete compressive strengths ranged from a low value of 21.2 to a high value of 67.4 MPa. For consistency, the specimen identification of various experimental data sets was established using the labels A1 through A20 while presenting single element FE results.

Table 1 Existing concrete compressive strength experimental data in the literature

Source	Specimen ID	f_c' (MPa)	Specimen re-labeled	Remark
Jansen and Shah (1997)	2.0	45	A1	H:D = 2, Fig. 7, pp. 31
Rokugo and Koyanagi (1992)	P-2	39	A2	H:W = 2
Ansari and Li (1998)	HS06	42	A3	Fig. 5, pp. 750
	HS10	69	A4	
Ren <i>et al.</i> (2008)	No label	45.3	A5	Fig. 8, pp. 552
		48.1	A6	
		49.5	A7	
		50.3	A8	
		54.7	A9	
		56.3	A10	
Yi <i>et al.</i> (2003)	w/c=0.69	21.2	A12	28 days, Fig. 1, pp. 1237
	w/c=0.54	33.8	A13	
	w/c=0.39	50.8	A14	
	w/c=0.30	67.4	A15	
	MS0	55.2	A16	
Saatci and Vecchio (2009)	SS0	50.1	A17	Fig. 3 (a), pp. 79
	SS1	44.7	A18	
	SS2	47.0	A19	
	SS3	46.7	A20	

In this study, nonlinear finite element software program ANSYS (ANSYS 2009) was employed as a preprocessor to create the mesh, and the geometry of single element model. LS-DYNA material models (Livermore Software Technology Corporation 2007a) were defined using LS-PrePost software program (Livermore Software Technology Corporation 2007b).

2.1 Element type

A three-dimensional eight-node brick element, Solid164, was used in ANSYS to model the concrete. At each node, the element has translations (u_x, u_y, u_z), velocities (v_x, v_y, v_z), and accelerations (a_x, a_y, a_z) in the nodal x, y and z directions. In explicit dynamic analyses v_x, v_y, v_z , and a_x, a_y, a_z are not essentially physical degrees of freedom (DOF). But their values are calculated as DOF solutions and stored for postprocessing. Reduced one point integration with viscous hourglass control was opted for Solid164 element for faster element formulation. Hourglass is a zero-energy mode with no physical meaning and generates a zigzag mesh form in the FE model. Solid164 element supports material and geometric nonlinearities in the explicit dynamic analysis.

2.2 Concrete material models

A number of concrete and concrete like brittle material models have been developed with various levels of complexity and accuracy. Pressure hardening, strain rate dependency, strain hardening, and equation of state are common key features for all material models. Concrete material models MAT16, MAT84, MAT72rel3 and MAT159 implemented in LS-DYNA are briefly discussed in here. These material models are typically used for vehicle road side concrete barrier crashworthiness safety analysis and for modeling of concrete structures subjected to shock and blast impulse loadings (Yonten *et al.* 2005, Tu and Lu 2009). Additional details on these material models are presented elsewhere (Livermore Software Technology Corporation, 2007a).

LS-DYNA MAT16 (MAT_PSUEDO_TENSOR) is a pseudo tensor geological model widely used in the simulation of concrete structures subjected to short duration impulsive loading. The model is implemented in two modes, namely, Response Mode I and II. Response Mode I is a simple tabular pressure dependent yield surface for standard geologic models as Mohr-Coulomb yield surface with Tresca limit. Response Mode II is a complex two yield surface versus pressure function with options to drift between lower and upper surface curves. Response Mode II concrete has further options to generate concrete material model parameters only by providing concrete compressive strength as a single input. Other parameters are internally generated as a function of concrete compressive strength.

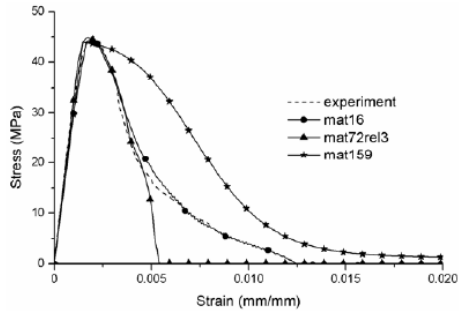
MAT72rel3 has three independent yield failure surfaces with shear dilation, and concrete damage surfaces. This plasticity model replaces tensile cutoff and provides a smooth transition to the residual failure. MAT72rel3 requires a total of 50 input data with option for automatic model generation by requiring the compressive strength of concrete as an input.

MAT84 is a smeared crack Winfrith concrete model implemented in the eight-node single integration point continuum element. The model yield surface expands with increasing hydrostatic stresses. The model radii at the compressive and tensile meridian are determined by locally rate sensitive compressive and tensile strengths. The flow stress is determined by the radial return to the yield surface and tensile failure is predicted if the maximum principal stress at yield is greater than half the current tensile strength. The model requires 32 input values and has also options for concrete model input parameter generation with the compressive strength of concrete as a single input.

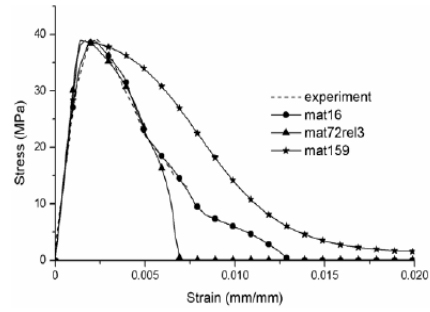
MAT159 is used to characterize the concrete behavior. The model is a smooth or continuous surface cap model developed by Federal Highway Administration (FHWA) to simulate the behavior of road side concrete barriers subjected to high dynamic loadings. It has a smooth intersection between the shear yield surface and hardening cap. The initial damage surface coincides with the yield surface. The rate effects are modeled with visco-plasticity. An element loses its strength and stiffness as damage accumulation is equal to unity. The model is mesh insensitive and maintains constant fracture energy regardless of the element size.

2.3 Single element model analysis results

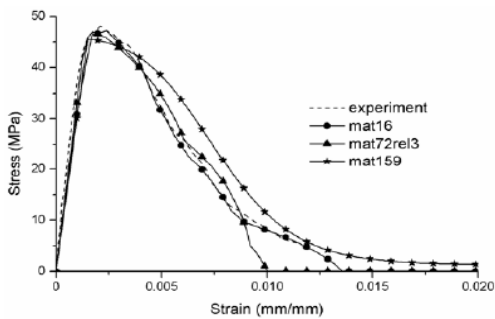
In Fig. 1, stress-strain curves of single element FEA models and the test specimens (A1-A20) are compared. Concrete material models MAT16, MAT84, MAT72rel3, and MAT159 which were previously defined as available options in LS-DYNA were employed in FEA simulation. MAT84 showed poor results in a preliminary analysis and subsequently was dropped from further



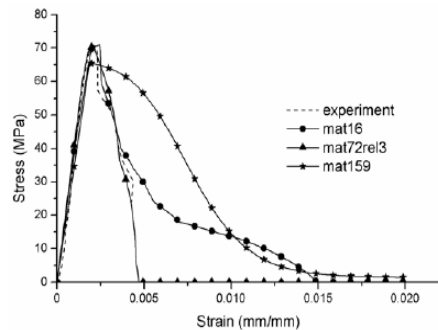
(a) Comparison with A1



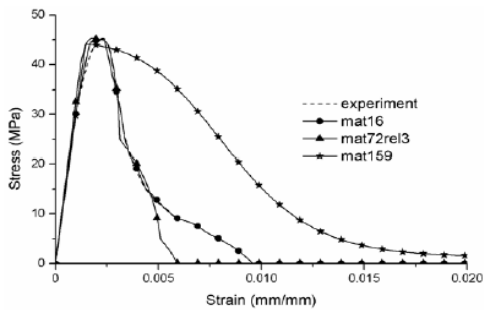
(b) Comparison with A2



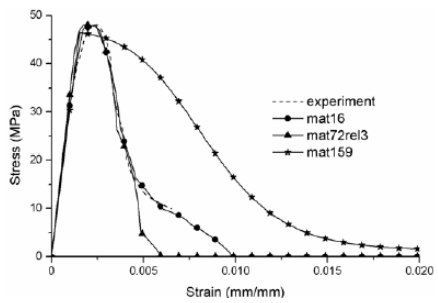
(c) Comparison with A3



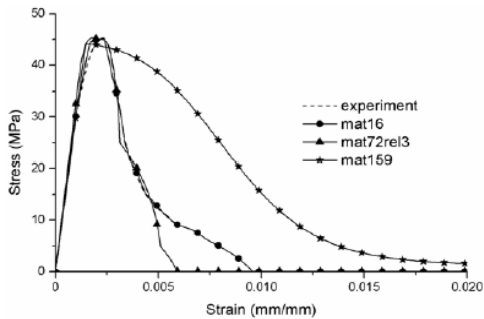
(d) Comparison with A4



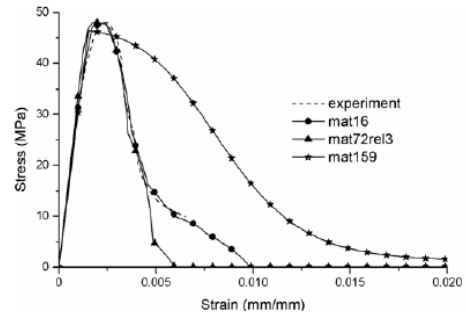
(e) Comparison with A5



(f) Comparison with A6

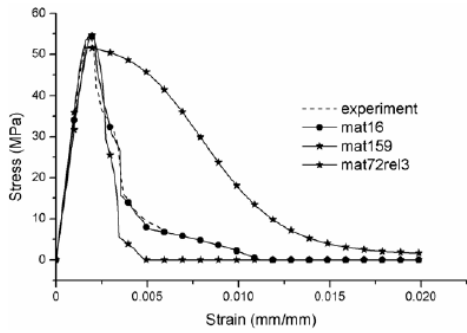


(g) Comparison with A7

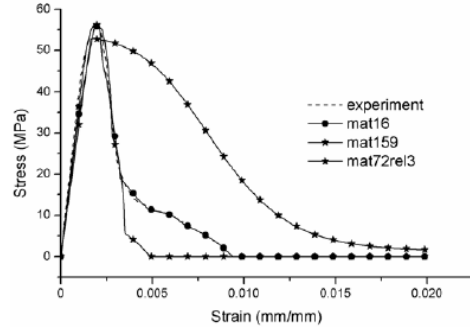


(h) Comparison with A8

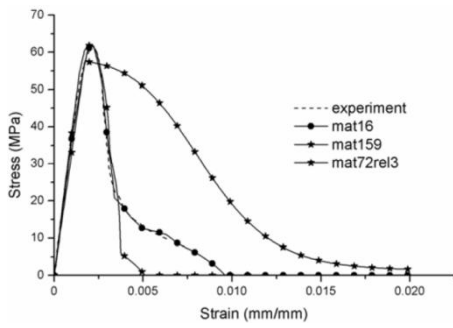
Fig. 1 Single element FEA and experiment results



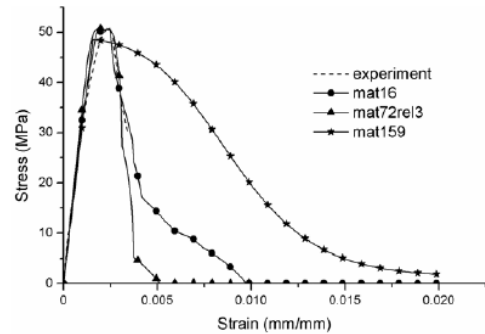
(i) Comparison with A9



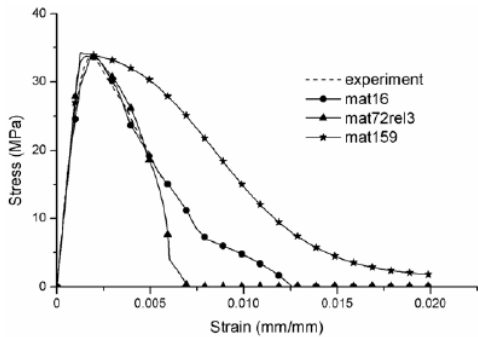
(j) Comparison with A10



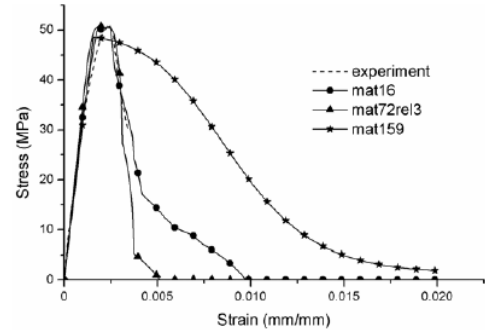
(k) Comparison with A11



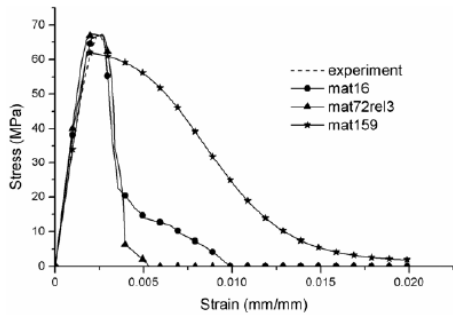
(l) Comparison with A12



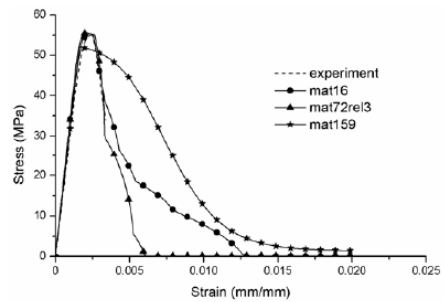
(m) Comparison with A13



(n) Comparison with A14



(o) Comparison with A15



(p) Comparison with A16

Fig. 1 Continued

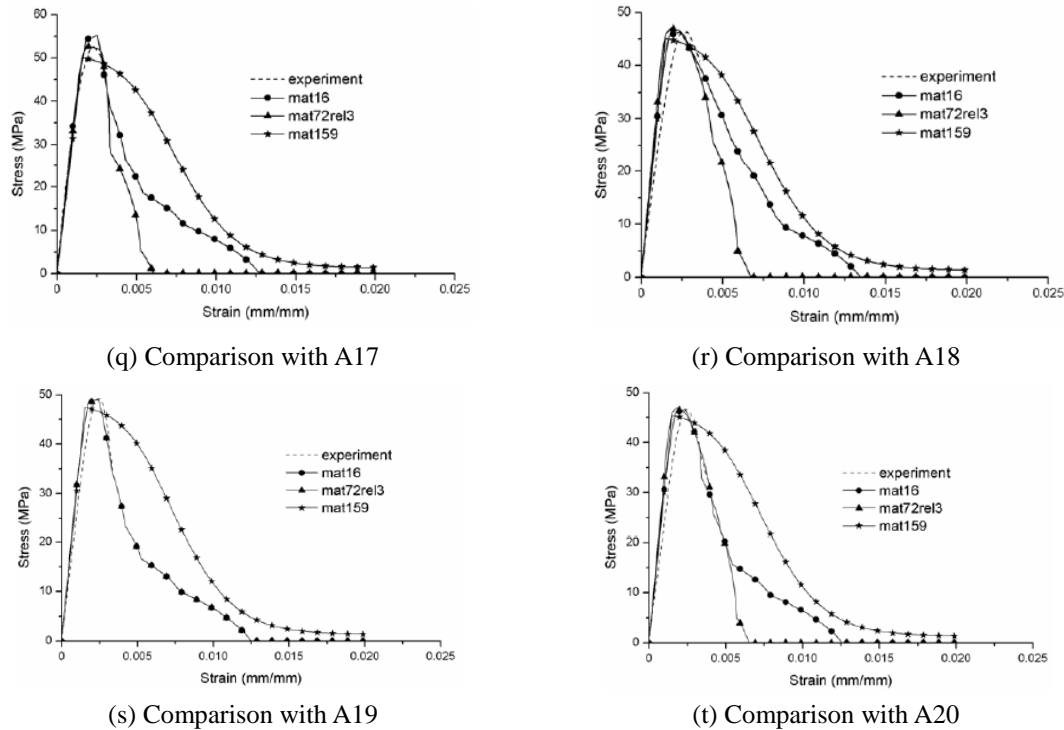


Fig. 1 Continued

consideration. The stress-strain curves of FEA models were in good agreement with those of the experiments in the ascending portion for all material models. However, for the descending portion of the curve, which is referred as the softening region, MAT16 outperformed other material models in terms of accuracy when compared to the experimental results. The upper region of descending branch of concrete stress-strain curves agreed well for MAT72rel3, while relatively slight deviation was observed in the lower portion of the descending curve. For MAT159, the concrete softening region showed relatively small deviation as compared to other material models. Overall, MAT16 agreed well with all experimental data both in ascending and descending portions of the stress-strain plots.

3. Development of the damage model

As mentioned earlier, determination of an accurate concrete damage model can significantly enhance the finite element analysis simulation results. Similar to concrete compressive stress-strain curves, damage scale factor versus effective plastic strain curves consist of ascending and descending regions. A statistical regression analysis was performed using damage scale factor and effective plastic strain values from calibrated single element models to propose an analytical concrete damage scale model. The proposed model characterized both the ascending and the descending regions of the concrete damage curve.

Fig. 2 shows the ascending branch of damage scale factor versus effective plastic strain curves.

The horizontal plateau formed at the peak concrete compressive strength was due to small divisions used for the horizontal axis and provided smooth softening transition between ascending and descending branches.

Eq. (1) represents the ascending branch of the concrete damage curve. The concrete damage model was derived through regression analysis using damage scale factor and effective plastic strain data of the twenty selected experiments shown in Table 1. The ascending branch of fourteen experimental data coincided with the proposed model.

$$\eta = 0.994 - 0.7027 \exp\left(\frac{-\lambda}{3.12 \times 10^{-7}}\right) \tag{1}$$

As compared to the descending branch, in the ascending branch, smaller divisions were employed particularly for the horizontal axis to be able to visualize the minute differences between the curves of damage scale factor (η) versus effective plastic strain (λ). Fig. 3 shows the descending branch of damage scale factor versus effective plastic strain curves. The twenty selected experimental curves from the six existing studies, namely A1 through A20, showed similar behavior pattern.

The proposed analytical model of descending branch of the concrete damage curve is presented in Eq. (2). The equation was derived using the mean plus standard deviation values from regression analysis of damage scale factor and effective plastic strain values of the twenty experimental data.

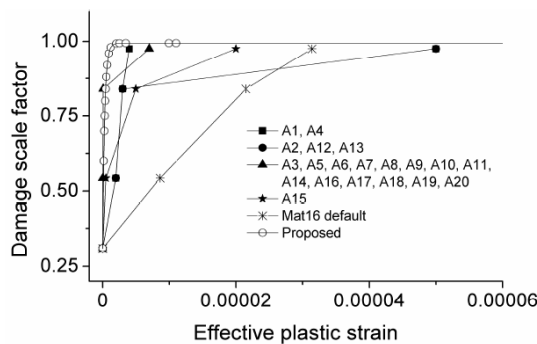


Fig. 2 Ascending portion of damage scale factor versus effective plastic strain curve

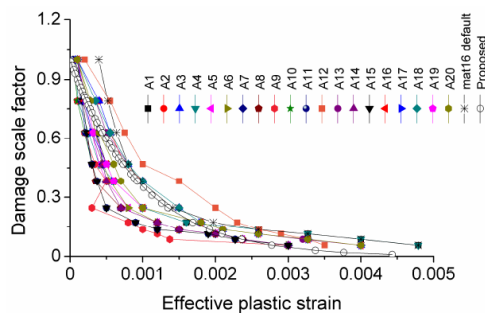


Fig. 3 Descending portion of damage scale factor versus effective plastic strain curve

Unlike default values of LS-DYNA software program, Eq. (2) is a function of concrete compressive strength (f'_c in MPa) resulting in a more accurate concrete damage scale factor.

$$\eta = \exp^{-1050\lambda \left(\frac{f'_c}{45}\right)^{0.15}} \quad (2)$$

Damage scale factor (η) values in Eqs. (1) and (2) vary from zero to one, where zero represents no concrete damage and one indicates that the element no longer carries any load due to severe damage. The range of concrete compressive strengths in Eq. (2) varies from 20 to 70 MPa. The user would be required to input the concrete compressive strength, in MPa and evenly distributed values of damage scale factor (η) ranging from zero to one; the proposed model automatically generates pairs of damage scale factor (η) and effective plastic strain (λ) values readily to be used as input for the material model.

In the following sections, the proposed analytical concrete damage scale model as given by Eqs. (1) and (2) was implemented into the finite element analysis model of full-scale vehicle bridge pier collision to validate its accuracy.

4. Case study: vehicle-pier collision simulation

Finite element analysis of a single hammerhead reinforced concrete bridge pier model subjected to vehicle impact load was performed to determine the accuracy of the proposed concrete damage model. Similar to single element, to model the bridge pier, Solid164 was used in ANSYS to model the concrete elements, and MAT16, MAT72rel3, and MAT159 of LS-DYNA were employed to model the concrete material while incorporating the proposed damage scale model.

Steel bars were modeled using a three-dimensional spar element, Link160. The geometry of the element is defined with one-node at each element end and additional orientation node at the element center. Link160 element has three degrees of freedom at each node for displacement, velocity and acceleration in x , y , and z directions. The element supports material and geometric nonlinearities and is compatible with the Solid164 brick element. LS-DYNA material model 3 (MAT_PLASTIC_KINEMATIC) was employed to model the steel material. Failure strain value of 0.16 was used to erode failed elements. It has the options to integrate rate effects and kinematic or isotropic hardening rules. Perfect bond assumption between the steel bars and concrete was forced by merging Link160 steel bar element nodes to coincide with Solid164 element nodes so that the two materials share the same nodes.

4.1 Mesh generation and boundary conditions

Due to complex reinforcement layout and full-scale FEA modeling, the single hammer pier column model development involved tedious mesh generation. Triangular prism wedge at the pier cap was modified into steps to accommodate the mapping process for tetrahedron solid element meshing. The reinforced concrete pier was fine meshed with the element sizes equal to 76.2 mm in the location of collision and 152.4 mm elsewhere to reduce the total number of elements and thus the computational time. The finite element model of reinforced concrete pier had a total of 82,264 solid, beam, link, and spring elements. In order to capture complete realistic vehicle impact response, beam and spring elements were employed for the piles and the soil, respectively. In-

plane x and y displacements at the top of the pier were restrained to zero.

Field crash test data of Chevy C1500 pick-up truck with a rigid barrier was employed to validate the FEA models of the pier (Mohammed and Parvin, 2010). Brief details of Chevy C1500 vehicle and single hammerhead bridge pier finite element models are presented in the next section.

4.2 Field crash test data and vehicle model

Chevy C1500 pick-up truck collision with rigid barrier field test was performed by the Transportation Center of Ohio (Test no. 1741). The field crash test data are available for download at National Highway Traffic Safety Administration website (2009). C1500 pick-up truck finite element model was developed and validated by the National Crash Analysis Center (NCAC) at the George Washington University for the Federal Highway Administration (FHWA) and National Highway Traffic Safety Administration (NHTSA) for crashworthiness analysis and further research. Chevy C1500 pick-up truck FE modeling involved disassembling of each vehicle part into components and three-dimensional geometry of each component was digitized by a passive arm connected to the computer. Thus, three-dimensional geometry of vehicle parts were imported and meshed into finite element models with high accuracy. Coupon tests from various parts of the vehicle were performed to characterize material properties of each part.

Zaouk *et al.* (2003) used C1500 pick-up truck crash field test data to validate the development of Chevy C2500 finite element model. C1500 pick-up truck was 4.3 L V6 whereas C2500 was 5.7 L V8 and weighted extra 300 kg as compared to C1500. The results of finite element simulation were found consistent with those of the crash tests. In the present study, detailed FE model of Chevy C2500 pick-up truck with 58,313 elements was used for the pier collision simulation.

4.3 Pier model

Figs. 4 and 5 show single hammerhead pier column dimensions, steel reinforcement details, and pile layout. The dimensions of the pier were obtained from AASHTO's LRDF Design Example Manual for Steel Girder Superstructure Bridge which was prepared by the Federal

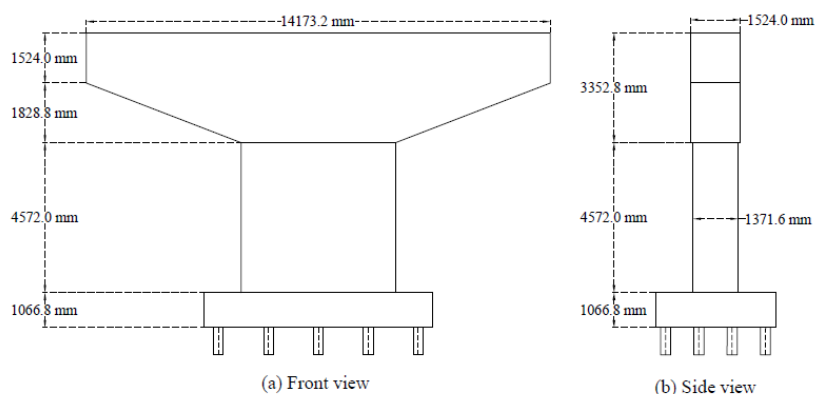


Fig. 4 Front and side views dimensions of the pier

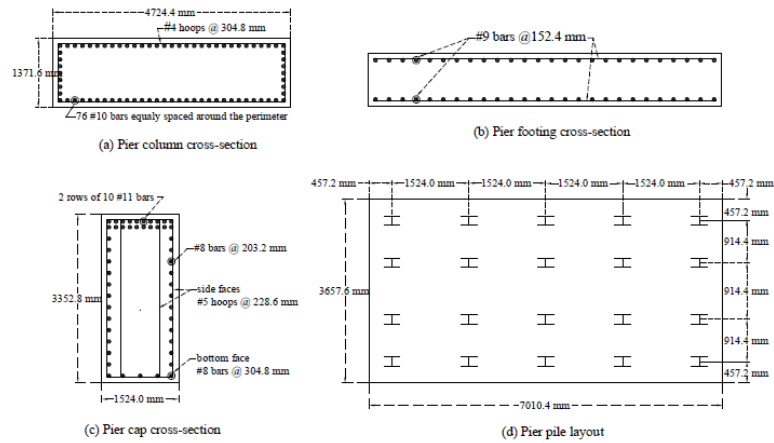


Fig. 5 Pier reinforcement details and pile layout

Highway Administration/National Highway Institute (AASHTO, 2003). The manual has detailed step-by-step design procedures with supplemental commentary, and considers multiple standard load combinations. Thus, the results reported in this paper can be easily reproduced by researchers and practicing engineers for further study.

4.4 Vehicle-pier simulation results

LS-DYNA single precision software program on Glenn (IBM 1350) Linux Cluster at the Ohio Supercomputer Center (OSC) was used to perform nonlinear explicit finite element analysis. The simulation run time duration for the pier vehicle collision analysis was 0.15 second using 12 processors. The total CPU time to complete each run was 50.5 hours. The explicit time step was 1E-8 second and the values of output parameters were given for every 1E-4 second. SAE-60 filter was employed to reduce the noise in the time history output.

In this section, comparative study of vehicle-pier collision FEA model using the proposed damage scale factor implemented in MAT16, MAT72rel3 and MAT159 is presented. FEA of vehicle pier collision with default damage scale factor using Mat16 is also shown for the sake of comparison.

Fig. 6 and Table 2 present Chevy C2500 dynamic force versus time history and peak dynamic impact force (PDIF) for MAT16, MAT72rel3 and MAT159 material models, respectively. Dynamic impact force versus time history response is critical in quantifying structural force demand during the vehicle bridge pier collision. The spikes in dynamic force versus time history plots were due to the effect of more rigid vehicle components (Fig. 6). Finite element results showed that for 56 km/hr vehicle approach speed, the single hammerhead pier column experienced only local damage at the location of collision with no global deformation. Comparison of field test data and FEA peak dynamic force using various material models indicated that MAT16 using the parameters of the proposed concrete damage scale model showed good agreement with a slight variation of 3.85%. With the exception of the peak value, the dynamic force versus time history curves had identical response behavior and shape for all material models. MAT16 with the proposed concrete damage model outperformed the other material models.

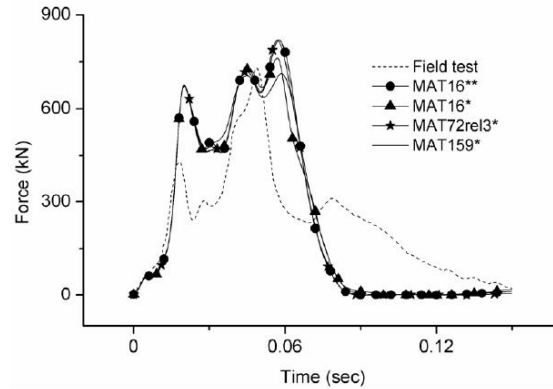


Fig. 6 Chevy C2500 vehicle FEA and field test impact force versus time history

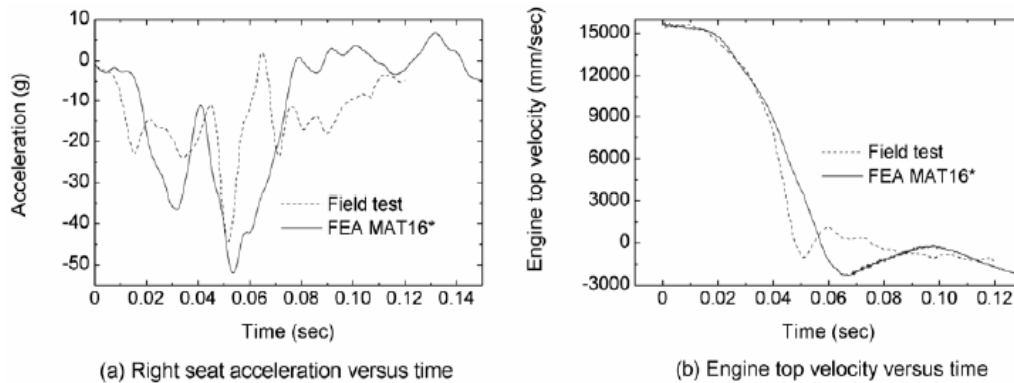


Fig. 7 Chevy C2500 vehicle acceleration and velocity versus time history

Table 2 Comparison of field test data and FEA of vehicle-pier collision results

Material ID	Peak dynamic impact force (N)	Difference(%)
Field test	732,155	--
Mat16**	820,120	10.73
Mat16*	761,510	3.85
Mat159*	711,727	-2.87
Mat72rel3*	819,107	10.62

*proposed damage scale model

**default parameter input

Fig. 7(a) presents comparison of the field test data and Chevy C2500 FEA acceleration versus time history results. The time history plots are extracted from FEA results of MAT16 using calculated parameters of the proposed concrete damage scale model. FEA peak right seat acceleration result had 14.7% deviation as compared to the field test data. The deviation might have been attributed to the existing 300 kg mass difference between the Chevy C2500

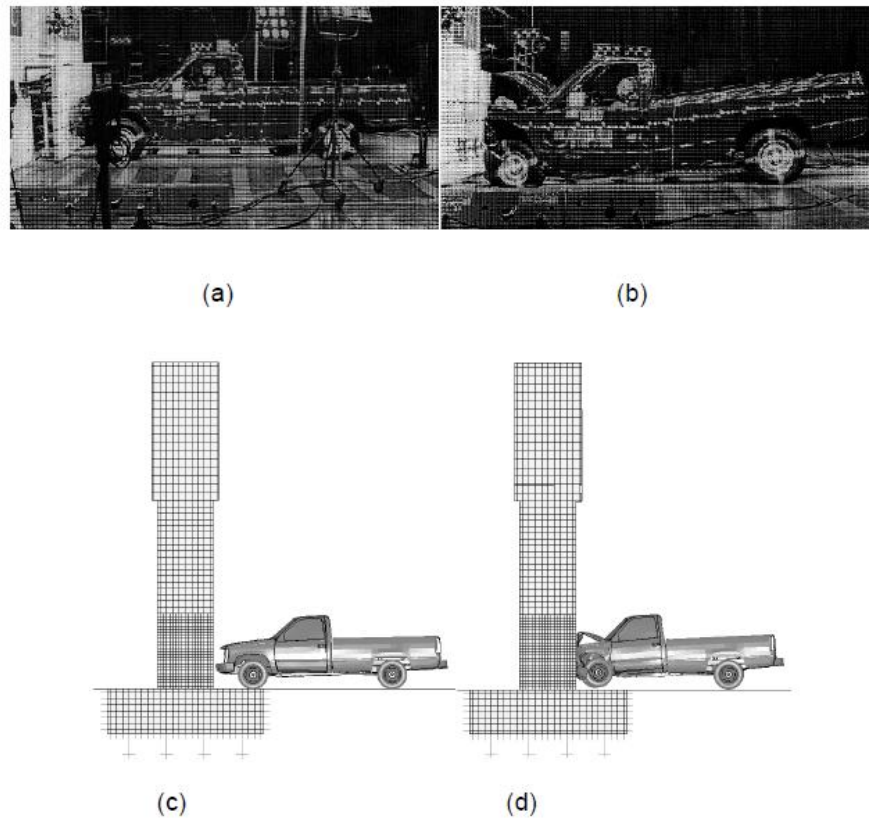


Fig. 8 Chevy C2500 vehicle collision (a) Pre-crash field test (b) post-crash field test (c) pre-crash FEA model (d) post-crash FEA model

vehicle employed in the FEA and Chevy C1500 vehicle used in the field crash test (Mohammed and Parvin 2010). In Fig. 7(b), the Chevy C2500 field test engine top velocity versus time history response was compared to that of FEA. Again there were good correlations for the maximum values and the shape of the curves.

Fig. 8 shows the pre and post-crash behavior of the field test and FEA of C2500 vehicle-pier collision. Finite element analysis results showed that single hammerhead pier column experienced only local damage at the location of collision with no global deformation. Images taken by high speed camera during crash test were visually compared to the FEA of vehicle-pier collision using the developed damage scale model. Similar vehicle damage was observed in the FEA models when vehicle collided with the pier at 56 km/hr approach speed identical to the field test.

5. Conclusions

In this paper a damage scale analytical model to characterize pre and post peak behavior of concrete material has been proposed. To formulate the damage scale model, single element models

followed by statistical regression were developed using numerous existing concrete compressive test data. Subsequently, the proposed damage scale model was used for concrete material models of LS-DYNA to simulate a full-scale reinforced concrete bridge pier subjected to vehicle impact loading. The response was compared to field crash test data from the collision of the truck with a rigid concrete barrier to validate its accuracy. Based on the results of this study, the following conclusions can be drawn:

- In the preliminary analysis, single element analysis demonstrated that the post peak behavior of concrete material was controlled by the concrete damage model.
- The proposed model improved the concrete softening behavior. Furthermore, use of the proposed model resulted in up to 50% reduction in the number of parameters that must be input by the user for the four concrete material model options in LS-DYNA.
- Field-test data and finite element analysis results of vehicle collision with single hammerhead pier showed the best agreement when using MAT16 with input parameters of the proposed concrete damage scale model as opposed to other material models (namely MAT72rel3, and MAT159 in LS-DYNA). This model was capable of accurately capturing the response of the reinforced concrete bridge pier subjected to vehicular impact.

6. Future work

The usefulness of the proposed damage model for a bridge pier under impact load was confirmed in this study. However, further investigation is suggested to examine the model for other types of structures and load scenarios. Moreover, developing a subroutine code to integrate the proposed damage scale into concrete material models in commonly used explicit nonlinear finite element analysis software programs would result in more accurate and efficient simulation by automatic generation of concrete material input data.

Acknowledgments

This work was supported in part by an allocation of computing time from the Ohio Supercomputer Center.

Reference

- AASHTO (2003), "*LRFD design example for steel girder superstructure bridge*", FHWA/NHI, Washington, DC.
- Ansari, F. and Li, Q.B. (1998), "High-strength concrete subjected to triaxial compression", *ACI Mater. J.*, **95**(6), 747-755.
- ANSYS, Inc. (2009), "*ANSYS users' manual*", Version 11, Canonsburg, PA.
- Buyukozturk, O. and Shareef, S.S. (1985), "Constitutive modeling of concrete in finite element analysis", *Comput. Struct.*, **21**(3), 581-610.
- Chung, Y.S., Meyer, C. and Shinozuka, M. (1989), "Modeling of concrete damage", *ACI Struct. J.*, **86**(3).
- Han, D. and Chen, W. (1987), "Constitutive modeling in analysis of concrete structures", *J. Eng. Mech.*, **113**(4), 577-593.

- Jansen, D.C. and Shah, S.P. (1997), "Effect of length on compressive strain softening of concrete", *J. Eng Mech. ASCE*, **123**(1), 25-35.
- Liu, Y. Huang, F. and Ma, A. (2011), "Numerical simulations of oblique penetration into reinforced concrete targets", *Comput. Math. Appl.*, **61**(8), 2168-2171.
- Livermore Software Technology Corporation. (2007a), *LS-DYNA users' manual*, Version 971, Livermore, CA.
- Livermore Software Technology Corporation (2007b), *LS-PREPOST 2.1 software program*, Livermore, CA.
- Livermore Software Technology Corporation (2012), *LS-DYNA: Keyword User's Manual-Volume II: Material Models*, Livermore, CA.
- Malvar, L.J., Crawford, J.E., Wesevich, J.W. and Simons, D. (1997), "A plasticity concrete material model for DYNA3D", *Int. J. Impact Eng.*, **19**(9), 847-873.
- Mohammed, T.A. and Parvin, A. (2010), "Vehicle bridge pier collision validation analysis and parametric study using multiple impact data", *FHWA Bridge Eng Conf.*, Orlando, FL. 287-294.
- Ren, X.D., Yang, W.Z., Zhou, Y. and Li, J. (2008), "Behavior of high-performance concrete under uniaxial and biaxial loading", *ACI Mater. J.*, **105**(6), 548-557.
- Rokugo, K. and Koyanagi, W. (1992), "Role of compressive fracture energy of concrete on the failure behavior of reinforced concrete beams", In: Carpinteri, A. editor. *Applications of fracture mechanics to reinforced concrete*. Elsevier, New York, NY, 437-464.
- Saatci, S. and Vecchio, F.J. (2009), "Effects of shear mechanisms on impact behavior of reinforced concrete beams", *ACI Struct. J.*, **106**(1), 78-86.
- Tu, Z. and Lu, Y. (2009), "Evaluation of typical concrete material models used in hydrocodes for high dynamic response simulations", *Int. J. Impact Eng.*, **36**(1), 132-146.
- Hu, H. and Schnobrich, W. (1989), "Constitutive modeling of concrete by using nonassociated plasticity", *J. Mater. Civ. Eng.*, **1**(4), 199-216.
- Yi, S.T, Kim, J.K. and Oh, T.K. (2003), "Effect of strength and age on the stress-strain curves of concrete specimens", *Cement Concrete Res.*, **33**(8), 1235-1244.
- Yonten, K., Manzari, M.T., Marzougui, D and Eskandarian, A. (2005), "An assessment of constitutive models of concrete in the crashworthiness simulation of roadside safety structures", *Int. J. of Crashworthiness*, **10**(1), 5-19.
- Zaouk, A.K., Bedewi, N.E., Kan, C.D. and Marzougui, D. (1996), "Validation of a non-linear finite element vehicle model using multiple impact data", *Int. Mechanical Eng. Congress and Exposition*, Atlanta, GA, 91-106.